OPEN ACCESS

University of BRISTOL

Link to publication record in Explore Bristol Research
PDF-document

University of Bristol - Explore Bristol Research

General rights

The Effect of Baseband Impedance Termination on the Linearity of GaN HEMTs

M. Akmal[†], J. Lees[†], S. Bensmida[*], S. Woodington[†], V. Carrubba[†], S. Cripps[†], J. Benedikt[†], K. Morris[*], M. Beach[*], J. McGeehan[*] and P. J. Tasker[†]

[†]*Cardiff School of Engineering, University of Cardiff, The Parade, Cardiff, CF24 3AA, Wales, UK*

[*]*Centre for Communications Research, University of Bristol, Woodland Rd, Bristol, BS8 1UB, UK*

AkmalM1@Cardiff.ac.uk

Abstract— **This paper demonstrates the significant effect of baseband impedance termination on the linearity performance of a 10W GaN HEMT device driven to deliver a peak envelope power of approximately 40dBm. The paper also proposes a further refinement to a state-of-art active IF load-pull measurement system to allow the precise independent control of all significant baseband components generated as a result of the multi-tone excitation used. The presentation of specific baseband impedances has delivered a 20dBc and 17dBc improvement in IM$_3$ and IM$_5$ inter-modulation products respectively, relative to the case of a classical, ideal short circuit. As expected for this device, this was achieved by emulating appropriate negative impedances lying outside of the Smith chart, and when this observation is considered alongside the Envelope Tracking PA architecture, this raises the interesting possibility of significantly improving PA linearity using the very mechanisms that are employed to improve PA efficiency.**

I. INTRODUCTION

The advent of fourth generation (4G) wireless systems, namely Long Term Evolution (LTE) and mobile WiMAX, has significantly increased the demand on Power Amplifier (PA) linearity requirements. For example, the PAs used in LTE systems, employing orthogonal frequency division multiplexing (OFDM) for downlink need to accommodate scalable bandwidths ranging between 1.4 MHz and 20 MHz [1]. In such wideband applications, any variation in baseband impedance over bandwidth can cause adverse effects in terms of device linearity performance where intermodulation distortion (IMD) levels can vary asymmetrically with instantaneous signal bandwidth - these problems are generally termed memory effects [2], [3].

Such problematic effects can lead to significant difficulty in achieving PA performance that meets the required linearity specifications. Indeed, if the intermodulation distortion becomes asymmetrical, then this can lead to different digital pre-distortion compesation requirements for lower and upper sideband IMD signals, which itself can be problematic. As a result, some common linearization techniques can be rendered ineffective because their success relies upon constant and equal intermodulation levels over the signal bandwidth [3]. Thus, it is of prime importance to understand these anomalous baseband impedance variation effects. To further investigate such baseband impedance effects on the linearity performance

of a device, two distinct measurement systems have been developed [4], [5] that can provide independent baseband impedance control. The general approach adopted in this work is to engineer actively the base-band impedance environment in order to achieve a modulation-frequency-independent impedance environment over a bandwidth of at least eight times that of the modulation bandwidth.

In earlier work [5]-[7], only the impedance presented to the two most significant baseband components (IF1 and IF2) generated as a result of 2-tone excitation were controlled. This was achieved by combining two, phase coherent arbitrary waveform generators (AWGs) whilst the device was driven at a relatively backed-off level at 1dB below the 1dB compression point. However, when the device is driven more deeply into compression, significantly more mixing terms are generated, and in order to achieve a sufficiently broadband IF termination significant modification of the baseband load-pull measurement system was required in order to accurately account for higher baseband harmonics.
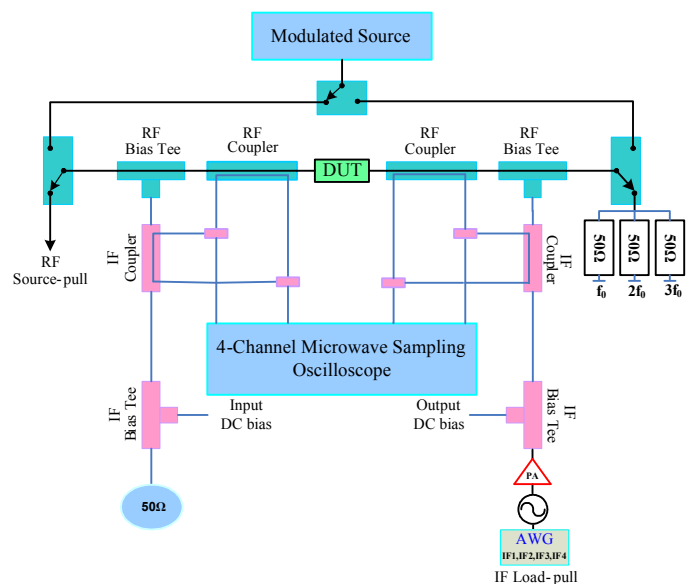

Fig. 1 Modulated waveform measurement system with active baseband load-pull.

The integrated measurement architecture depicted in Fig. 1 provides the ability to present independent, baseband impedances to all the significant IF frequency components that result from a multi-tone excitation. This is now achieved in the time domain using a single arbitrary waveform generator (AWG) to synthesise the necessray waveforms to allow a constant and specific IF impedance environment to be maintained across a wide IF bandwidth.

The initial aim of this paper is to confirm and demonstrate that baseband electrical memory effects can be greatly reduced by terminating the baseband impedance into ideal short circuits: an impedance environment that would result from conventional design and the use of video bypass capacitors. The second part of the paper considers 'if' and 'how' this situation can be improved by considering alternative baseband impedance conditions. As expected, for the GaN device considered, and for this degree of compression, the measured linearity significantly improves when negative baseband impedances are presented. Although such impedances are non-realiseable using conventional, passive designs, this is not the case when active, baseband injection architectures such as Envelope Tracking (ET) are employed.

II. LINEARITY INVESTIGATION AND ANALYSIS

All the measurements presented in this section are for a CREE CGH40010 discrete 10W GaN HEMT device, characterised at the centre frequency of 2GHz, within a custom 50Ω test fixture. This fixture was calibrated over a relatively wide 50 MHz baseband bandwidth, and over 100 MHz RF bandwidths centred around fundamental, second and third harmonics, with both baseband and RF calibrated reference planes established at the device's package plane. This allowed the accurate and absolute measurement of all the significant voltage and current spectra generated at the input and output of the device.
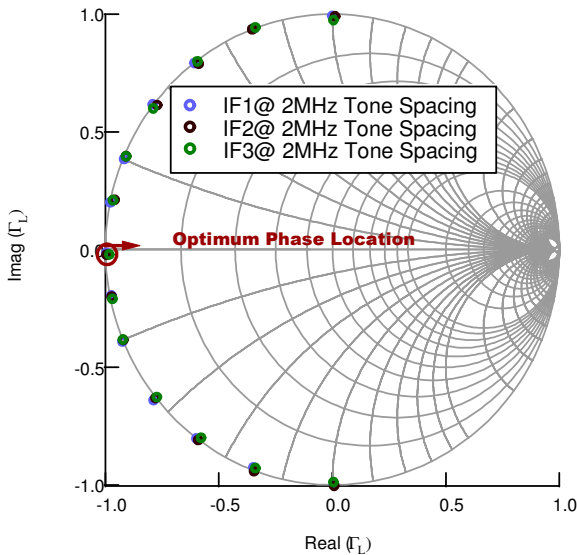

Fig. 2 Measured IF impedances at 2MHz tone spacing using IF active load-pull.

Two-tone measuremens were performed using a 2MHz tone spacing, with the device class-AB biased. Respective drain and gate bias voltages of 28V and -2.05V resulted in a quiescent drain current of 250mA ($I_{DSQ} \cong 5\%\ I_{DSS}$). The device was driven into approximately 1.5dB of compression whilst delivering 39.5dBm output peak envelope power (PEP) with fundamental and harmonic components terminated into a nominal impedance of 50Ω, at both the input and the output.It should be noted that braodband 50Ω load is used to simplify the required measurement architecture. Although this is non-optimal, but is considered sufficiently representative for the linearity anaylsis presented here. Active IF load-pull was then used to synthesise a range of IF reflection coefficients in order to quantify the effects of the low frequency, broad-band IF load impedance termination on the non-linear behaviour of the DUT.

Fig. 2 illustrates a measurement where the phase of the IF1, IF2 and IF3 loads were varied simultaneously, in steps of 15° around the perimeter of the Smith chart, whilst keeping the magnitude of IF reflection co-efficient at unity. The results depicted in Fig. 3 clearly show that, as expected, there exists a strong dependence of IM3 and IM5 magnitude on the phase of the baseband impedance. The results explicitly identify an expected optimum phase in the region of 180° for IF1, IF2 and IF3 loads, where IM3 and IM5 distortion products are minimised.
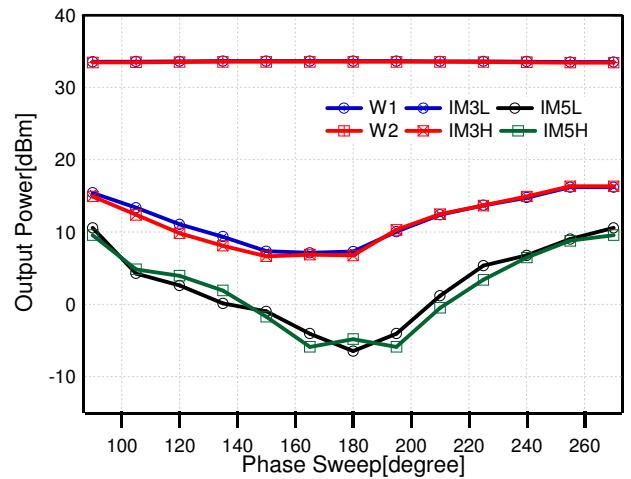

Fig. 3 Measured fundamental and IMD magnitudes at 2MHz Tone Spacing as a function of IF1, IF2 and IF3 phase.

The measured inter-modulation distortion products presented in Fig. 3 show that when a perfect short impedance ($\Gamma_{IF}=1\angle180°$) is presented to the significant baseband components, the measured IM3 and IM5 magnitudes can be seen to be -24dBC and -38dBC respectively.

Active load-pull however has an important advantage in that it is able to seamlessly synthesise both positive impedances within the Smith chart, as well as negative impedances outside the Smith chart. So, in order to explore further the optimum baseband impedances for best linearity conditions, the broadband IF impedance was swept over a

measurement grid, including the short circuit condition, and extending some way outside the Smith chart. $IM3_L$ and $IM5_L$ contours were then plotted and are shown in Fig. 4 and Fig. 5 respectively, and in both cases show a purely resistive negative optimum impedance. The optimum $IM3_L$ performance (point B) is found to be -43.5dBc, and is approximately 19.5dBc better than the case where usual short circuit is provided to all the significant baseband components (point A).
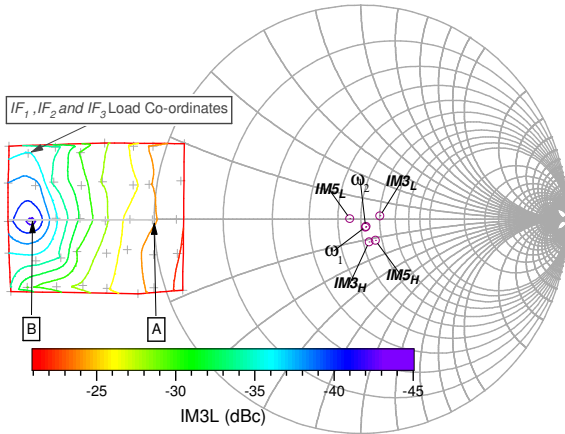

Fig. 4 Measured $IM3_L$ linearity contours as a function of IF1, IF2 and IF3 loads.

With regard to the $IM5_L$ and $IM5_H$, an improvement of 17dBc was achieved at an optimum termination (point C) as compared to the short circuit case (point A). As the contours for $IM3_L$ and $IM3_H$ were found to be almost identical, as was the case for $IM5_L$ and $IM5_H$, only $IM3_L$ and $IM5_L$ contours are presented here.
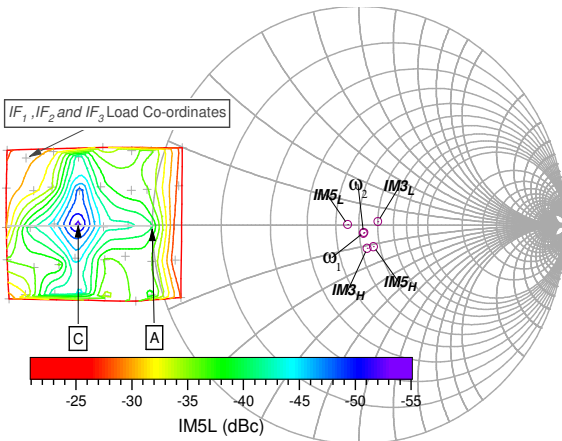

Fig. 5 Measured $IM5_L$ linearity contours as a function of IF1, IF2 and IF3 loads.

If we consider the behaviour of IM3 and IM5 components for the cases of IF loads only located along the real axis, it can be seen that with regard to Fig. 6, the real baseband impedances required to minimize IM3 and IM5 are different, and located at points B and C respectively. Establishing the

broadband IF load at point B leads to an approximate 11 dB degradation in the established IM5 optimum. Conversely, fixing the IF load at point C results in an approximate 7dB degradation from the established IM3 optimum. Having said this, it can be seen that adopting a broadband IF load impedance between points B and C offers a significant improvement in linearity when compared to the usual short circuit termination located at point-A.
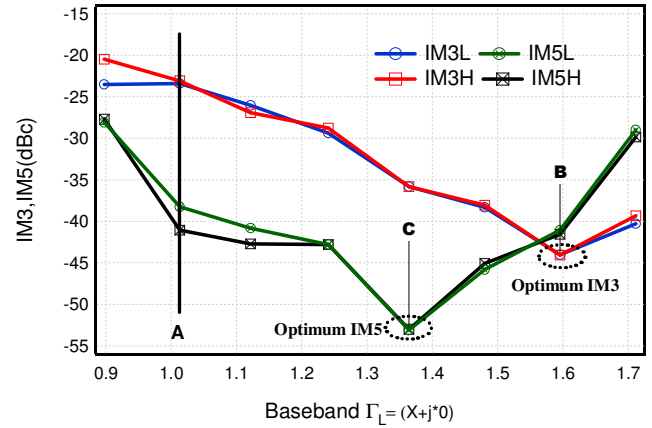

Fig. 6 Measured IM3 and IM5 linearity as a function of baseband reflection coefficient (Γ_L).

Fig. 7 shows the baseband voltage waveforms that result when the IF impedances for point A, B and C are presented to the device.
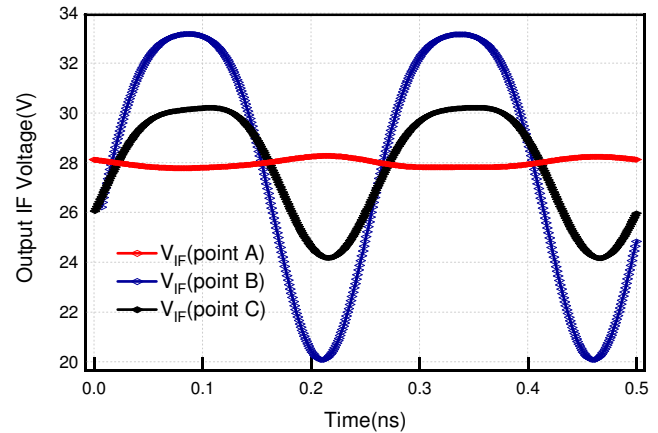

Fig. 7 Baseband voltage that result for the two cases of IF load impedances for minimum IM3 and IM5.

III. OPTIMIZED DEVICE LINEARITY PERFORMANCE

From the previous two-tone measurements, it was clear that for this device, the optimum baseband impedance for linearity resides outside the Smith chart. To investigate this observation further and specifically, to explore the possibility of linearization through the direct application of an ET voltage waveform, additional measurements were carried out for three different cases of DC drain voltage (V_{dc}): 28V, 24V and 16V.

The device was deep class-AB biased, and driven approximately 2.5dB into compression with fundamental and harmonic components again terminated into a passive 50Ω load. Using a symmetrical 3-tone, 100% AM excitation signal cantered at 2 GHz with an envelope frequency of 2 MHz, a different IF load condition was used for each case of V_{dc}: for the case of V_{dc}=28V, an ideal short circuit termination was synthesised for each of the four significant baseband components, resulting in a near static supply rail. The slight 'ripple' that remained was associated with IF5, but this was very small and in the order of 200 mV_{p-p}, so was considered not to be of concern. For the second case of V_{dc}=24V, a sufficiently negative resistance was presented to all four IF components to result in an $8V_{p-p}$ baseband voltage being developed. For the third case of V_{dc}=20V, the IF load was again adjusted such that a $16V_{p-p}$. baseband voltage waveform was developed.

Fig. 8 shows how in each case, the injected baseband signals track the RF input signal envelope and provide an 'ET-like' variable supply voltage to the device. It is also clear that for the three cases, the peak baseband voltage is the same at 28V, thus allowing meaningful comparison. For the case of V_{dc}= 28V, an average drain efficiency of 38.1% was achieved at a peak envelope power (PEP) of 39.72dBm. For the case of V_{dc}=24V, the average drain efficiency was 41.5% at a PEP of 40.3dBm.
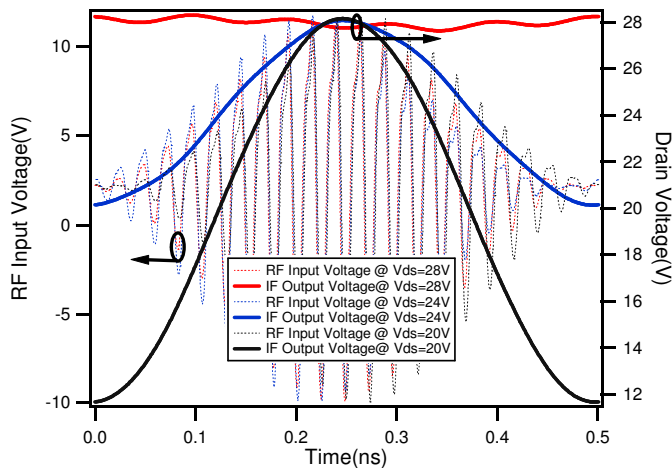

Fig. 8 Measured dynamic IF voltage envelops in-phase with input RF voltages

A slightly better performance in terms of efficiency and output power was achieved with V_{dc}=20V. Therefore, applying a dynamic drain voltage has increased the achievable peak output power, and has thus enabled a higher efficiency than was possible with a fixed supply voltage of 28V. Linearity performance is summarized in Table-1, where it is shown that for the case of V_{dc}=20V, IM3 and IM5 distortions are suppressed by 10dBc and 3dBc respectively compared to the static V_{dc}=28V case where a short circuit impedance was maintained for all four IF components. For the case where

V_{dc}=24V, only a small improvement in IM3 distortions was observed along with an 8 dBc improvement in IM5 distortion.

TABLE I
THREE TONES MEASURED LINEARITY RESULTS FOR
THREE DISTINCT DRAIN VOLTAGES

Supply Voltage(V)	IM5L dBc	IM3L dBc	W1 dBm	Wc dBm	W2 dBm	IM3H dBc	IM5H dBc
28	-35.68	-12.83	27.85	35.69	28.02	-13.12	-36.47
24	-43.05	-15.86	28.08	35.18	28.15	-16.37	-43.26
20	-38.95	-22.81	28.39	34.39	28.49	-22.57	-39.41

VI. CONCLUSION

Linearity investigations of 10W GaN HEMT under modulation excitations have shown that for the device considered, the optimum impedance for best linearity lies outside the Smith chart. Interestingly, the results also suggest that there exists separate optimum impedances for suppression of IM3 and IM5 distortion products.

Additionally, application focused measurements with non-optimal load (50Ω) have shown that efficiency as well as linearity can be improved at reduced drain supply voltages: for V_{dc}=20V, the average drain efficiency is improved by approximately 5% together with an improvement of 10dBc in IM3 when compared to the static V_{dc}, where short circuit impedance was maintained for all four baseband components.

REFERENCES

[1] 3GPP Long Term Evolution specification, [Online]. Available: http://cp.literature.agilent.com/litweb/pdf/5989-8139EN.pdf
[2] Joel Vuolevi and Timo Rahkonen, "Distortion in RF Power Amplifiers," Norwood, MA: Artech House, 2003
[3] J. Vuolevi, J. Manninen, and T. Rahkonen, "Cancelling the memory effects in RF power amplifiers," in *IEEE Int. Symp. Circuits and Systems*, pp. 57–60, 2001.
[4] Spirito, M. , Pelk, M.J. , van Rijs, F. , Theeuwen, S.J.C.H., Hartskeerl, D. , de Vreede, L.C.N. , Active Harmonic Load–Pull for On-Wafer Out-of-Band Device Linearity Optimization," *IEEE Trans. Microw. Theory Tech.*, vol. 54,no. 12, pp. 4225-4236, Dec. 2006.
[5] Alghanim, A.; Lees, J.; Williams, T.; Benedikt, J.; Tasker, P "Using active IF load-pull to investigate electrical base-band induced memory effects in high-power LDMOS transistors," in *Proc. Asia-Pacific Microwave Conference*, 2007, 11-14 Dec. 2007 Page(s):1 - 4.
[6] Alghanim, A;Less, J.; Williams, T.; Benedikt, J.; Tasker, P. "Reduction of electrical base-band memory effects in high-power LDMOS DevicesUsing Optimum Termination for IMD3 and IMD5 using active load-pull", in Proc., *IEEE International Microwave Symposium*, June 2008.
[7] J. Lees, et al, "Demystifying Device Related Memory Effects Using Waveform Engineering and Envelope Domain Analysis", *in Proc. 38th European Microwave Conference*, October 2008.